

Article

Particulate Matter versus Airborne Viruses—Distinctive Differences between Filtering and Inactivating Air Cleaning Technologies

Andrea Burdack-Freitag^{1,*}, Michael Buschhaus¹ , Gunnar Grün^{1,2}, Wolfgang Karl Hofbauer¹ , Sabine Johann¹, Anna Maria Nagele-Renzl¹, Andreas Schmohl¹  and Christian Rudolf Scherer¹ 

¹ Fraunhofer Institute for Building Physics (IBP), Fraunhoferstraße 10, 83626 Valley, Germany

² Institute for Acoustics and Building Physics, University of Stuttgart, Pfaffenwaldring 7, 70569 Stuttgart, Germany

* Correspondence: andrea.burdack-freitag@ibp.fraunhofer.de

Abstract: The current pandemic of the SARS-CoV-2 virus requires measures to reduce the risk of infection. In addition to the usual hygiene measures, air cleaners are a recommended solution to decrease the viral load in rooms. Suitable technologies range from pure filters to inactivating units, such as cold plasma or UVC irradiation. Such inactivating air cleaners, partly combined with filter technology, are available on the market in various designs, dimensions and technical specifications. Since it is not always clear whether they may produce undesirable by-products, and the suitability for particular applications cannot be assessed on the basis of the principle of operation, the effectivity of six inactivating devices was investigated in a near-real environment. The investigations were based on a standard method published by the VDI. The procedure was extended in such a way that a permanent virus source was simulated, which corresponds to the presence of a person suffering from COVID-19 in a room. The study addresses the difference of the mere presence of viruses to the determination of the virulence. As a result, a deep understanding is provided between the behavior of a virus as a pure aerosolized particle and its real infectivity in order to enable the assessment of suitable air cleaners.

Keywords: virus inactivating air cleaner; plasma technology; UVC; virulence; VOC; ozone



Citation: Burdack-Freitag, A.; Buschhaus, M.; Grün, G.; Hofbauer, W.K.; Johann, S.; Nagele-Renzl, A.M.; Schmohl, A.; Scherer, C.R. Particulate Matter versus Airborne Viruses—Distinctive Differences between Filtering and Inactivating Air Cleaning Technologies. *Atmosphere* **2022**, *13*, 1575. <https://doi.org/10.3390/atmos13101575>

Academic Editor: Stefan Schumacher

Received: 9 August 2022

Accepted: 22 September 2022

Published: 27 September 2022

Publisher's Note: MDPI stays neutral with regard to jurisdictional claims in published maps and institutional affiliations.



Copyright: © 2022 by the authors. Licensee MDPI, Basel, Switzerland. This article is an open access article distributed under the terms and conditions of the Creative Commons Attribution (CC BY) license (<https://creativecommons.org/licenses/by/4.0/>).

1. Introduction

During the COVID-19-pandemic caused by the novel virus SARS-CoV-2, new technologies have appeared on the market to reduce the viral load in indoor environments. Because their function is so new and not yet fully understood, the study focused on the microbial and chemical effectiveness of virus inactivating (disinfecting) technologies and the possible undesired by-products formed during operation. Acoustic properties and energy consumption were not considered since these parameters have already been collected by the manufacturers and not relevant for the study's aim. Pure filter technologies were also not investigated, as their mode of operation and side effects are established. Nevertheless, their differences to the inactivating technologies were described for deeper understanding since some air cleaning devices contain both technologies—inactivating units and filters.

The different mode of action of both technologies can be explained by the structure and biology of the virus. The SARS-CoV-2 virus has a single-stranded RNA genome of approximately 30,000 bases in length and forms bodies with a diameter of approximately 80–140 nm. In addition to the nucleoprotein structure, it has an envelope formed by a phospholipid bilayer with spike proteins, which enable docking to a host cell. An active virus (virulent) initiates the virus replication. The optimal environmental conditions for reproduction are ambient temperature and humidity [1–6].

Filter technologies have no influence on the infectivity of a virus; rather, the effectiveness of a filtering air cleaner in a room depends, on the one hand, on the properties of the filter medium used and, on the other hand, on the design details of the device. Impaction, interception, diffusion and electrostatic attraction are the relevant physical processes describing the deposition of aerosol particles on filter media, but no disinfecting processes take part. Usually, the ultra-fine particle filter classes ISO ePM1 and HEPA/ULPA H13, H14, U15 to U17 are capable of efficiently filtering out virus particles in the order of 0.1 to 0.3 μm . [7–10]. Its capability is quantified by determining the clean air delivery rate (CADR) under particular boundary conditions.

The effectiveness of an inactivating process on airborne viruses is essentially determined by the level of virulence, which means the remaining probability to infect a host. Studies with surrogate viruses comparable to corona viruses have shown good predictive power for successful decontamination and disinfection procedures to reduce the virulence of SARS-CoV-2-contaminated air [11–13].

Apart from some special technologies (e.g., photocatalysis and ionization radiation), two commercially available methods are able to reduce virulence: plasma technology and UVC radiation [14–17].

The first involves irradiation by cold ionizing plasma (also called non-thermal plasma, air ionization or dielectric-barrier discharge) formed by electrostatic discharge in the kilovolt range between different electrodes, which demonstrates a high virucidal effect [14,18–21].

In the further text, the term “plasma” is used as a synonym for cold plasma technologies. This technology has already been established for VOC reduction in indoor air, for surface and water sterilization and is also used for disinfection in food processing and the medical field [22–26]. Recent studies have also indicated an effective reduction in the virulence of airborne viruses. The effect of plasma treatment on microorganisms lies in the immediate oxidative attack on the cell membrane of bacteria and the protein capsid of viruses and the destruction of DNA or RNA by the reactive components [21,27–29]. Because of the short exposure times and relatively low plasma temperatures, few reaction products of concern and residual ozone have been identified so far. The risk of ozone release can also be minimized by capturing potential ozone with activated charcoal filters [30–34]. The use of activated carbon filters can reduce one advantage of inactivating technologies compared to filtering devices, namely, the much lower pressure drop and the resulting energy savings.

The second irradiation method uses UV radiation (ultraviolet radiation; wavelength range 100–380 nm). UV radiation is short-wave electromagnetic radiation that cannot be perceived by the human eye. It is divided into the following: UVA, 315–380 nm; UVB, 280–315 nm; and UVC, 100–280 nm. All UV ranges have a disinfecting effect. The UVC range from 200 to 280 nm exhibits by far the highest antimicrobial and antiviral efficacy, as these wavelengths are in the range where nucleic acids are particularly absorptive. UVC light inactivates RNA and DNA through the dimerization of two adjacent uracil bases. By destroying their nucleic acids, microorganisms are effectively inactivated; this works particularly well with viruses, as they have no means of repairing damage to their nucleic acids. Consequently, the optimal RNA absorption is between 240 and 280 nm, with maximum absorption at 260 nm [35–39]. For an effective reduction in aerosolized coronavirus activity, D90 radiation doses (UVC dose which inactivates 90% of active viruses) at a minimum of 3.7 J/m² and a maximum of 10.6 J/m² are necessary. In aqueous media, significantly higher radiation doses (37 J/m²) are required [16,40].

Since SARS-CoV-2 is a highly pathogenic virus in humans classified as a safety risk level 3 pathogen, realistic scientific investigations and tests directly using this virus as a target component are not possible outside strictly monitored laboratories requiring biosafety protection level 3. Therefore, replacing SARS-CoV-2 with a nonpathogenic surrogate virus represents the most reliable model according to the current technologies. Bacteriophage MS2 (*Emesvirus zinderi*) is often cited as an alternative; however, its smaller structure, a capsid without an additional lipid envelope, is less analogous to SARS-CoV-2 than human pathogenic noroviruses (these also without an envelope). Phi6 (*Pseudomonas phage phi6*)

and coronaviruses have similar characteristics in terms of shape (spherical) size (diameter approximately 85 nm), structure (enveloped virus), spike proteins, viral RNA genome (ssRNA–SARS-CoV-2; dsRNA–phi6), and environmental preferences [41–45].

Comparing the sensitivity of Phi6 and coronaviruses in an aerosol, the log₁ (D₉₀, which is the dose necessary for 90% inactivation) was determined to be 5–7 and 3.7–10.6 J/m², respectively. Phi6-phages are a very applicable surrogate for coronaviruses in aerosol experiments [38,40,46–52].

The focus of the study was to demonstrate the efficacy of inactivating technologies against a very high viral load, partially combined with filter technologies. The different reduction pathways between filtering of virus particles and reduction of the virulence was investigated. Potential undesired side effects as the formation of the by-products volatile organic compounds (VOC) and ozone were elucidated.

2. Materials and Methods

The investigations were based on the VDI expert recommendation VDI EE 4300-14 issued in September 2021 [17], which was introduced to standardize the testing of the effectiveness of air purification devices in room environments. Particular emphasis was placed on the comparability of the devices and the technologies in terms of effectiveness in a realistic environment for reducing the virus load and the comparability of different technologies. Deviating therefrom, the investigations were carried out among a permanent virus injection into the room throughout the tests, in contrary to spot dosing in the standard, to elucidate the realistic efficiency by a constant virus-emitting person.

Two fans ran only during the injection phase before switching on the air cleaners to ensure a homogenous virus concentration in the entire room. They were switched off during the air cleaners' operation. Then, the air mixing was only performed by the devices. An additional support by fans does not correspond with reality.

Therefore, the setup differed from the normative requirements for the calculation of the CADR for filtering air cleaners or HADR (hygienic air delivery rate) for inactivating devices [17,53]. Instead of that, the determination of the air cleaner loss coefficient k_{AC} and the natural loss coefficient k_{nat} was implemented by an evaluation model that is based on Equation (1) and consists of various calculation segments [54–56]. Each segment represents a characteristic part of the concentration curve and corresponds to a phase of the analyzed experiment. The concentration $c_n(t)$ at a certain time t was calculated by Equation (1) with the concentration $c_{n-1}(t_{n-1})$ at the end of the previous phase $n-1$, the source s_n of the phase n and the total loss coefficient k_n of the phase n :

$$c_n(t) = \frac{s_n}{k_n} + \left(c_{n-1}(t_{n-1}) - \frac{s_n}{k_n} \right) \cdot e^{-k_n \cdot (t - t_{n-1})} \quad (1)$$

In this model, the total loss coefficient k_n is the sum of the natural loss coefficient k_{nat} and, if applicable, the air cleaner loss coefficient k_{AC} . Dependent on whether the particle or Phi6 plaque forming unit concentration is the target quantity, either the parameter $k_{AC,particle}$ or $k_{AC,Phi6}$ is determined, respectively.

Six air cleaning devices with different inactivating units on basis of plasma or UVC technology were examined. Some of them were assembled with coarse and/or ultra-fine particle filters. One pure plasma device (1_P) and one with coarse and ultra-fine particle filters and an activated charcoal filter (2_P) were used. The UVC units were operated with UVC sources emitting wavelengths greater than 220 nm. UVC device 4_UV used an UVC source that emitted a discrete wavelength of 254 nm. Only in devices 2_P and 6_UV were ultra-fine particle filters installed. Table 1 provides an overview of the diversity of the investigated technologies.

Table 1. Investigated air cleaner.

Device No.	Inactivating Unit	Additional Assembly
1_P	Plasma	-
2_P	Plasma	Coarse filter, ultra-fine particle filter, activated charcoal filter for ozone reduction
3_UV	UVC (wavelength > 220 nm)	-
4_UV	UVC (discrete wavelength 254 nm)	-
5_UV	UVC (wavelength > 220 nm)	Coarse filter
6_UV	UVC (discrete wavelength 254 nm)	Ultra-fine particle filter

The test setup followed a realistic scenario to a continuous emitter in the room which simulated a continuous exhalation of viruses by an infectious patient. Non-pathogenic Phi6-bacteriophages with similar structure and environmental behavior as SARS-CoV-2 were injected into a controlled test environment. The investigations were conducted in the Fraunhofer Indoor Air Test Center (IATC) which is a unique climate-controlled test facility of about 129 m³ room volume (8.24 × 5.06 × 3.09 m³), where the indoor climate was specifically set and kept constant over the measurement period. Relative humidity was set to 40% RH, the room temperature to 19 °C. The test room was equipped with chairs, tables and dummies to simulate the situation within an occupied class room or an office. The air cleaners were positioned in the room in accordance with the specifications given by the manufacturers.

A nebulizer (AGK 2000, Co., Palas, Karlsruhe, Germany) was used to aerosolize the Phi6-bacteriophage suspension into room air at 1.5 bar inlet pressure. Dosing was initially performed for 1 h without turning on the device to generate a high viral load in the room. Then, the dosing and air cleaner were operated simultaneously to determine the virus phage reduction.

This experimental setup ran for a total of approximately 2 h. Particle concentrations in the sub-micron range (2.5 nm to 3 µm, adjustable to different particle sizes) were measured using a water-based condensation particle counter (WCPC 3788, Co., TSI, Buckinghamshire, UK) and an alcohol-based ultrafine particle counter (20 nm to 1000 nm, adjustable to different particle sizes, P-Trak; Co., TSI, Buckinghamshire, UK). Particle number concentration, temperature (OM-24, Co., Omega, Deckenpfronn, Germany), humidity (OM-24, Co., Omega, Deckenpfronn, Germany), and ozone concentration (O341M, Co. ansysco, Karlsruhe, Germany) were continuously recorded throughout the run.

The aerosolized phages were collected on gelatin filter (Co., Sartorius Stedim) with an air sampler (MBASS30V3, Co., Umweltanalytik Holbach with 50 L/min, Wadern, Germany) for 30 min each at 30, 65, and 95 min after the start of dosing, with a total volume of 1.5 m³. Subsequently, microbial analysis of the virulent phages was performed in the laboratory. During each test, reference measurements of the virus titer within the liquid before and after the test (about 3 × 10⁹ to 4 × 10¹⁰ PFU/mL, “plaque forming units, pfu”) were carried out to record the natural decrease in the test viruses and to account for this in the results. Additionally, the Phi6 background concentration in the air before switching on the Phi6 aerosol injection was determined.

A plaque assay method (according to [17,57–59]) was used to determine the concentration of collected active (virulent) phages. The uncertainty of the plaque assay is approximately 10–30%. The study results represent approximate values. An exact mathematical analysis of the results is available in [60]. The resulting plaques were counted and extrapolated to the sampled air volume concentrations. For statistical reasons, only the plates of the dilution steps with approximately 30–100 visible plaques were counted, according to the most probable number method (MPN) or dilution assay [61].

In parallel, air samples for VOC analysis were taken at 0–60 and 65–125 min on Tenax-TA/Carboxen 1003 adsorbers (Co., Supelco, Taufkirchen, Germany) with 0.1 L/min and dinitrophenyl hydrazine (DNPH, Co., Waters, Eschborn, Germany) silica cartridges for the analysis of aldehydes and ketones with 1 L/min. Sampling was performed in duplicate with a total volume of 2 and 5 L for VOCs and 60 L for selected aldehydes and ketones. Subsequently, the loaded adsorbents were subjected to instrumental analysis. The sampling strategy for airborne pathogen collection and VOC sampling was carried out, taking the recommendations given in ISO 16000-1 [62] into account.

The air samples on the Tenax adsorbers were analyzed by thermal desorption/gas chromatography-mass spectrometry (TD/GC-MS, TD100 (Co., Markes, Offenbach am Main, Germany), GC2010, and 2010 Ultra (Co., Shimadzu_Duisburg, Germany)). DNPH cartridges were extracted with acetonitrile. The extracts were analyzed for the hydrazones of aldehydes and ketones by high-performance liquid chromatography equipped with a diode array detector (HPLC-DAD). Identification of VOCs by TD/GC-MS was based on in-house reference measurements or the NIST database (Mass spectrum database of the National Institute of Standards and Technology, NIST14 and 14s). Quantification was performed using an in-house standard and toluene equivalent. Aldehydes and ketones were identified and quantified by HPLC-DAD analysis using in-house reference measurements [63].

The principal time schedule for all dosing and samplings was as follows:

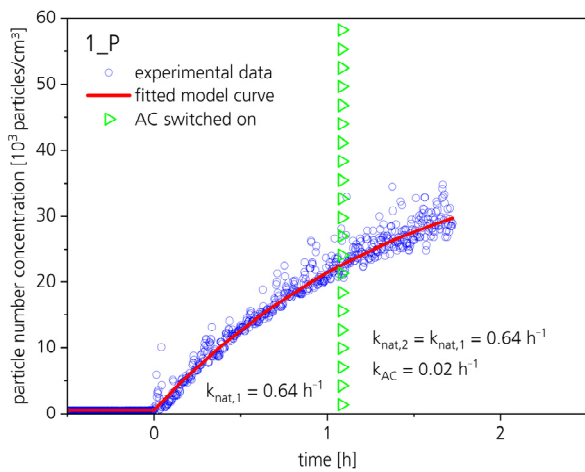
- –30–0 min: Background germ sampling P0 without injection.
- 0–60 min: Dosing for 1 h without switching on the device to generate a high viral load in the room.
- 0–60 min: First VOC sampling (background without air cleaner operation).
- 30–60 min: First germ sampling P1 (reference without air cleaner operation).
- >60 min: Dosing and air cleaner were operated simultaneously to determine phage reduction.
- 65–125 min: Second VOC sampling (during operation).
- 65–95 min: Second germ sampling P2 (first half hour during operation).
- 95–125 min: Third germ sampling P3 (about 1 h during operation).

3. Results

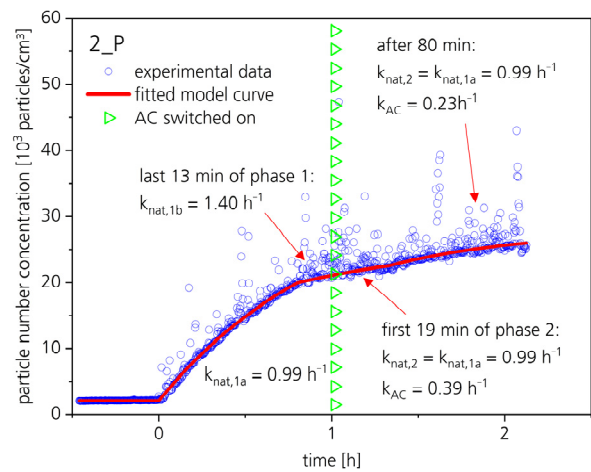
The particle concentration in the room, the virulence and the investigation of the by-products (e.g., ozone and VOCs) were considered separately. The final virulence efficiency depended on the particle concentration (filtration and/or sedimentation after switching on the devices), Phi6-bacteriophage half-life in air, and microbial-measured virulence. Device 1_P consisted of a plasma unit without any assembled filters or activated charcoal. This device released high amounts of ozone during the measurements, so the ozone concentration for the safe operation was exceeded. Therefore, the test had to be terminated earlier. Due to these circumstances, the results for that ozone-producing device have to be considered as orientating.

3.1. Particle Concentration

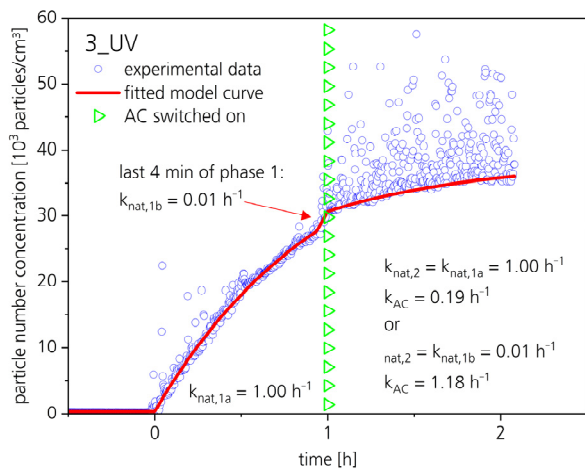
The inactivating air cleaning devices were exposed to a continuous dosing of the virus aerosol. After 1 h dosing time, the air cleaners were switched on. The particle curve progressions depended on additional assembly with fine particle filters. Figure 1a–f illustrates the particle concentration curves for all measured air cleaning devices.



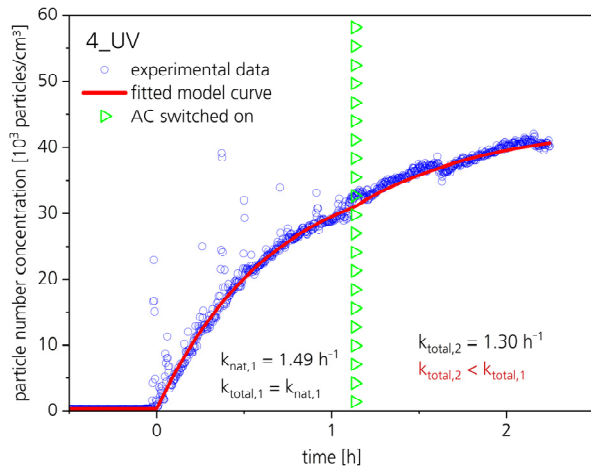
(a)



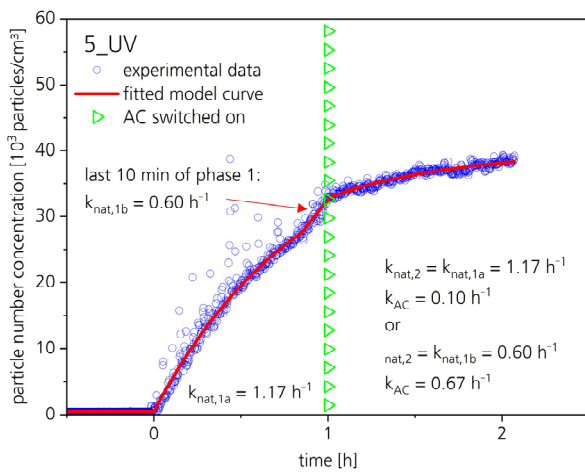
(b)



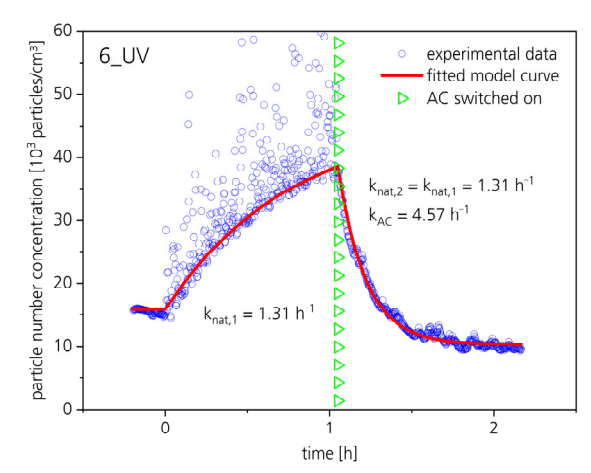
(c)



(d)



(e)



(f)

Figure 1. (a–f) Particle curves for all measured air cleaners and calculated loss coefficients k_{nat} and k_{AC} for particles (calculation see [54]).

During the entire phage dosing time, the particle concentration in the room was recorded with two particle counters for different particle size ranges. The first particle counter measured the ultra-fine particle range from 20 to 1000 nm (nano-scale), within which the freely moving, non-agglomerated 120 nm spherical Phi6-bacteriophages were covered. The second particle counter measured the ultra-fine and fine particle range from 2.5 nm to 3 µm (micro-scale), covering the agglomerated or hydrated Phi6-bacteriophages. The concentration curves were recorded, and $k_{AC,particle}$ was determined by an evaluation model based on Equation (1). In the initial phase, which means aerosol injection without an air cleaner, the particle concentration increased continuously. When the air cleaner was switched on, only for the air cleaner 6_UV a decrease in the particle concentration was observed. The natural loss coefficient during this measurement was 1.31 h^{-1} (determined for the initial phase) and the total loss coefficient during the phase with the active air cleaner was 5.88 h^{-1} . Therefore, the determined $k_{AC,particle}$ for 6_UV was 4.57 h^{-1} , which corresponds to a reduction of 89.8% in 30 min (compared to the VDI requirements [17] for an analogous setup without continuous aerosol injection). The devices 1_P and 4_UV did not reduce the particle concentration increase, thus $k_{AC,particle}$ was zero or almost zero ($<0.02 \text{ h}^{-1}$). For the devices 2_P, 3_UV and 5_UV, a slight reduction in the particle concentration increase was detectable, corresponding to a $k_{AC,particle}$ between 0.1 and 0.7 h^{-1} . Thus, only air cleaner 6_UV had a high cleaning efficacy concerning particles.

3.2. Efficiency in Reducing Virulence

The viral activity was determined using a plaque assay. The results of the plaque assay reflected the ability of the sampled particles to infect a host organism. The microbiological or hygienic loss coefficient $k_{AC,Phi6}$ of the air cleaner for bacteriophage Phi6 was determined by an evaluation model based on Equation (1) [54].

While dosing Phi6-bacteriophage into the room, three sampling events were performed. The first sample (P1) at the end of the initial phase (only aerosol injection, no air cleaner) was utilized for normalization, thus P1 equaled 100%. After switching on the air cleaner, two subsequent air samples (P2 and P3) were collected. Table 2 shows the normalized virus activity for all devices.

Table 2. Measured virulence at the different sampling times (P1 to P3). The phage concentration at the sampling time P1 is set as 100%.

Sample	Virulence [%] *					
	1_P	2_P	3_UV	4_UV	5_UV	6_UV
P1	100	100	100	100	100	100
P2	17.8	18.6	100	22.9	20.1	39.5
P3	- **	48.6	51.2	28.7	25.9	0.6

* Virulence is the quotient of P2 or P3 to P1. ** Sampling at time point P3 could not be performed because the test had to be aborted due to unacceptably high ozone concentrations.

Figure 2 illustrates the measured plaque forming unit concentrations at the sampling points P1, P2 and P3 and three calculated curves for each air cleaner. The curves were calculated analogous to the evaluation model for virus-inactivating air cleaners by surrogate virus plaque assay [54]. Sample P1 was used for normalization, thus the mean concentration of air sample P1 equals 100%.

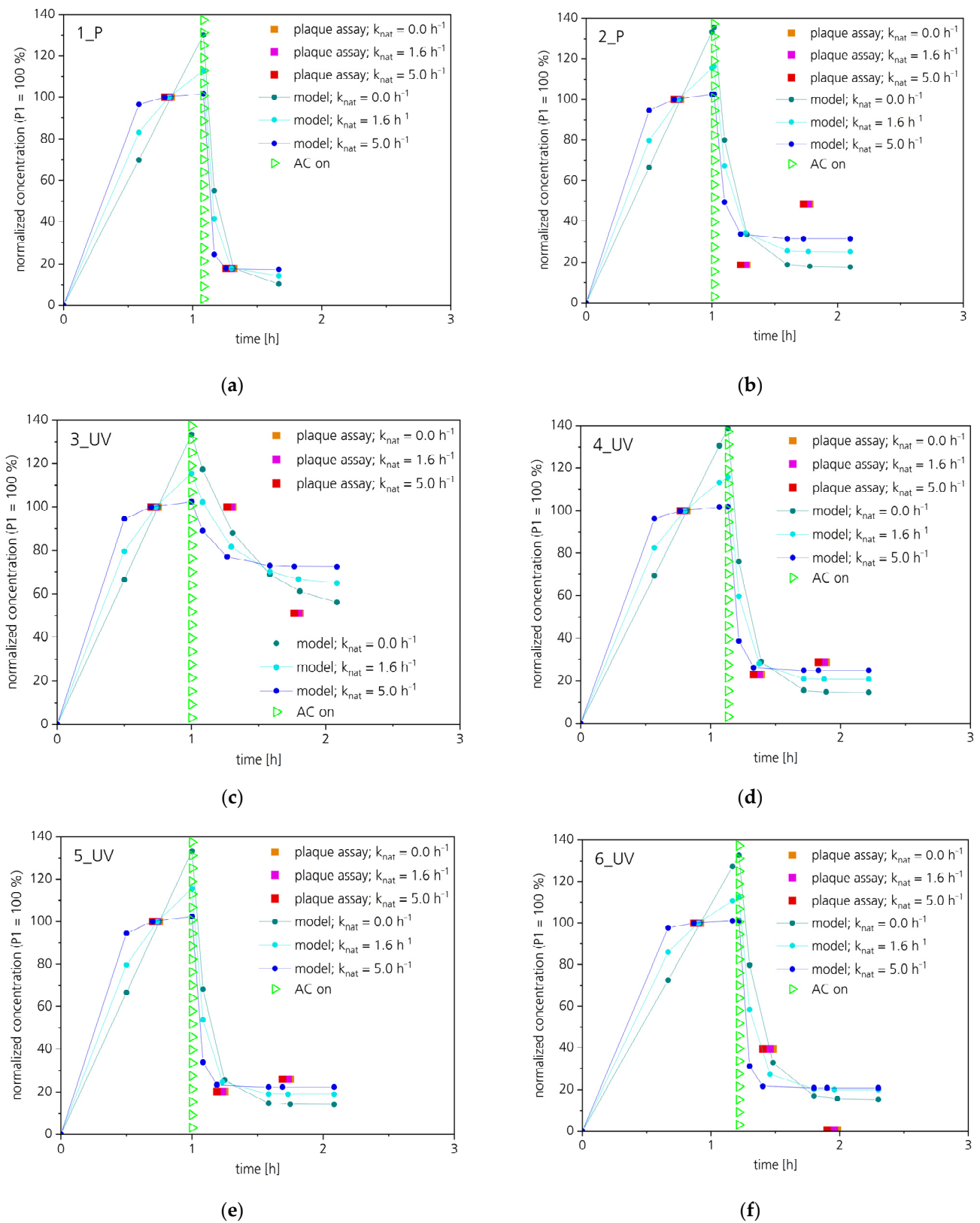


Figure 2. (a–f) Plaque assay fitting curves for the six measured air cleaners. Phi6 aerosol was released during the whole test procedure. An evaluation model based on Equation (1) was used for the calculation of the fitting curve.

The $k_{AC,Phi6}$ and $k_{AC,particle}$ values for all six devices are displayed in Figure 3. Due to the normalization by the plaque assay result of air sample P1, the normalized steady-state concentration that will be reached in operating phase usually is higher if the natural loss coefficient k_{nat} is higher. Therefore, for higher k_{nat} (grey column in Figure 3), the determined $k_{AC,Phi6}$ is also higher. Furthermore, due to the continuous injection of Phi6 aerosol in combination with the utilized normalization by sample P1, the parameter k_{nat} has only a minor effect on the parameter $k_{AC,Phi6}$ (see purple, orange and blue columns in Figure 3). Additionally, the parameter k_{nat} in the test room was determined by reference measurements (not shown). Usually, the parameter k_{nat} was in the range between 0.5 and 1.6 h^{-1} (purple or blue columns in Figure 3, respectively). The minimum value for $k_{AC,Phi6}$ ($= k_{AC,Phi6,min}$) that can be derived from the plaque assay data was determined by variation of k_{nat} until the lowest value for $k_{AC,Phi6}$ was reached.

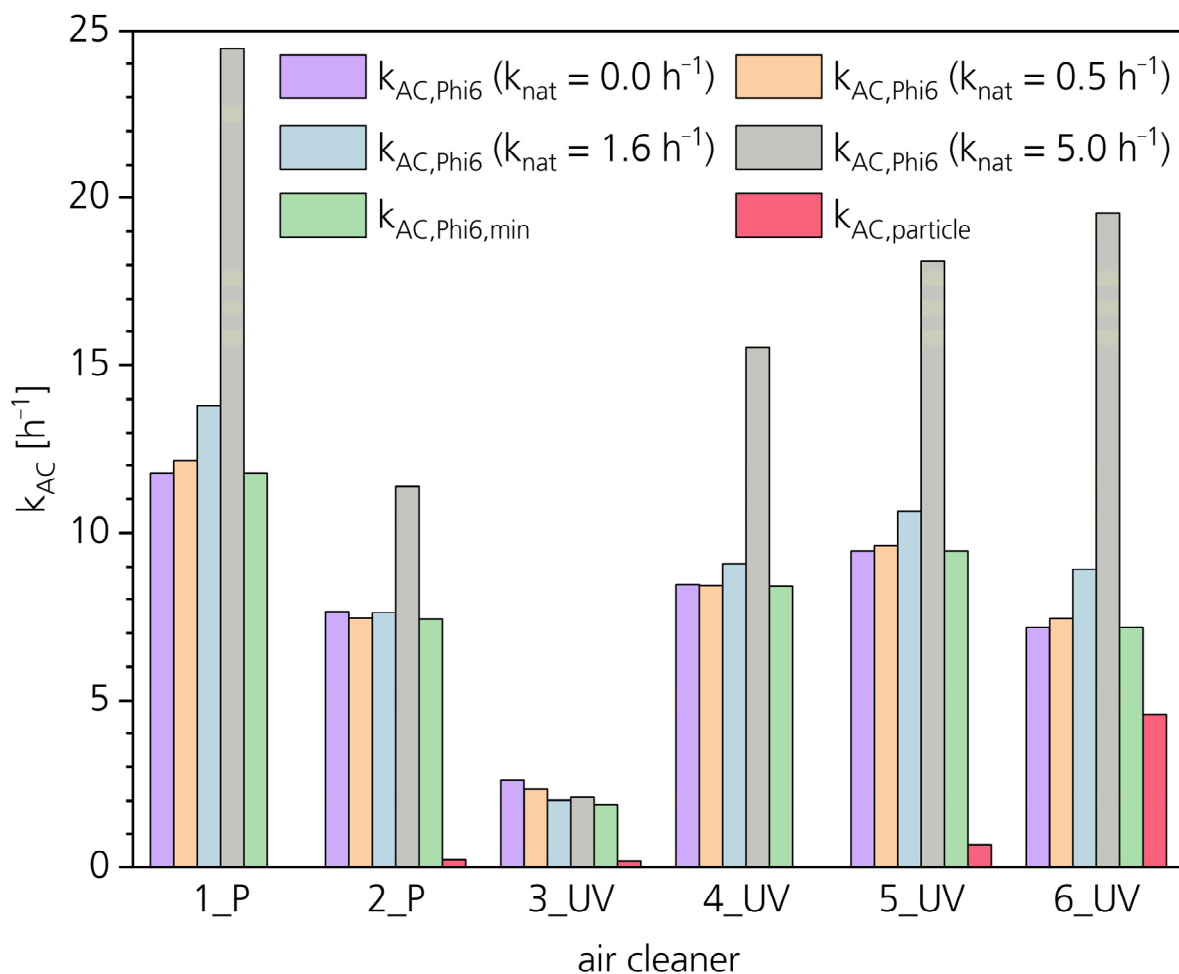


Figure 3. Air cleaner loss coefficients $k_{AC,Phi6}$ and $k_{AC,particles}$ for all six air cleaners determined by the evaluation model according to [54] based on Equation (1) for four different values of parameter k_{nat} . The loss coefficients $k_{AC,Phi6,min}$ of the air cleaners are the lowest $k_{AC,Phi6}$ values that could be received by variation of the parameter k_{nat} .

3.3. By-Products

According to the expert recommendation of the VDI [17] which is based on the requirements of the German environmental protection agency [64] and the European Centre for Disease Prevention and Control [65] one of the criteria for the use of air purification devices for the reduction of viruses is the proof that no harmful by-products, such as ozone and VOCs, are generated as reaction products when using plasma and UVC technology.

3.3.1. VOCs

Device operation raises the theoretical possibility that harmful reaction products may be formed from indoor emissions, degraded virus particles, or device components. Therefore, the room air was analyzed for VOCs (including selected aldehydes and ketones) before and during device operation. In some cases, the initial VOC concentrations in the test room were higher than the measured values during device operation (values not published).

Concentration values given in the LCI list [66] were used as decision criteria. These values were derived for emission test chamber experiments. Since the tests described are a special form of test chamber experiment, it seemed appropriate to use the LCI values (lowest concentration of interest) as a decision criterion. Table 3 shows the measured VOC concentrations of the six air cleaning devices compared with the LCI value. Initial values were already taken into account or mathematically deduced. None of the tested devices released any harmful reaction products, while concentrations of VOCs, aldehydes, and ketones were well below these limits.

Table 3. VOC release during operation.

Identified VOC	Device No.—Concentrations [$\mu\text{g}/\text{m}^3$] ¹						LCI [$\mu\text{g}/\text{m}^3$] ²
	1_P	2_P	3_UV	4_UV	5_UV	6_UV	
Acetaldehyde	- ³	- ³	- ³	- ³	- ³	- ³	300
Acetic acid	- ³	- ³	- ³	4	- ³	- ³	1200
Acetone	17	- ³	- ³	51	- ³	- ³	120,000
Acetophenone	4	- ³	- ³	- ³	- ³	- ³	490
Benzaldehyde ⁴	6	- ³	- ³	- ³	- ³	- ³	90
Benzoic acid ⁴	19	- ³	- ³	- ³	- ³	- ³	n.s. ⁵
Butanal	- ³	- ³	- ³	- ³	- ³	- ³	650
Decanal	2	- ³	- ³	- ³	- ³	- ³	900
Ethanol	54	- ³	- ³	2	- ³	- ³	n.s. ⁵
Heptanal	- ³	- ³	- ³	1	- ³	- ³	900
Nonanal	- ³	- ³	- ³	- ³	- ³	- ³	900
Octanal	1	- ³	1	- ³	- ³	- ³	900
1,2-Propanediol	- ³	- ³	1	- ³	- ³	- ³	3400
Toluene	- ³	- ³	1	- ³	- ³	- ³	2900

¹ formed VOCs during air cleaning in operation (difference between device switched on and switched off). ² Lowest concentration of interest. ³ “-” not detected. ⁴ Presumably source VOC-sampling onto TenaxTA[®]—degradation of adsorber material due to ozone reactions during operation. ⁵ “n.s.” not specified.

3.3.2. Ozone

The ozone concentration in the room was monitored over the entire period of the study. Potential ozone formation during operation of the air cleaners could thus be recorded directly and with time resolution. Table 4 shows the maximum ozone concentrations in the test room during operation of the air cleaning devices and, if applicable, the steady-state concentration for infinite run-time calculated by the model based on Equation (1).

Table 4. Ozone releases during operation. The ozone concentration when the air cleaner was switched on was subtracted from the maximum concentration.

Device No.	1_P	2_P	3_UV	4_UV	5_UV	6_UV
Measured maximum ozone concentration rise [$\mu\text{g}/\text{m}^3$]	583	4.0	2.8	0.2	8.5	1.0
Calculated maximum ozone concentration rise [$\mu\text{g}/\text{m}^3$]	1940	4.1	- ¹	- ¹	20.7 ²	- ¹

¹ A concentration decline occurred at the end of the measurement instead of a concentration rise. ² Ozone concentration rise started already before switching on the air cleaner; therefore, at least a part of the concentration rise might be due to ozone from outside.

The maximum ozone concentrations in the test room for the examined air cleaning devices with inactivating technologies ranged from 0 to almost $600 \mu\text{g}/\text{m}^3$. In accordance with the VDI expert recommendation [17] most of the technologies examined fell significantly below the tolerable residual ozone concentration of $10 \mu\text{g}/\text{m}^3$. Device 5_UV released with up to $24 \mu\text{g}/\text{m}^3$ slightly higher concentrations than the tolerated increase.

The plasma-based air cleaner 1_P released an extremely high amount of ozone. The measurements for this device were aborted at $586 \mu\text{g}/\text{m}^3$ for workplace safety reasons. Figure 4 illustrates the ozone concentration for all air cleaners. The concentration rise of air cleaner 1_P is conspicuous. The release rates of the air cleaners 2_P and 5_UV are similar, but due to the activated charcoal filter of 2_P the loss coefficient k is higher and therefore the steady-state concentration $c_{\text{steady state}}$ is lower than for device 5_UV.

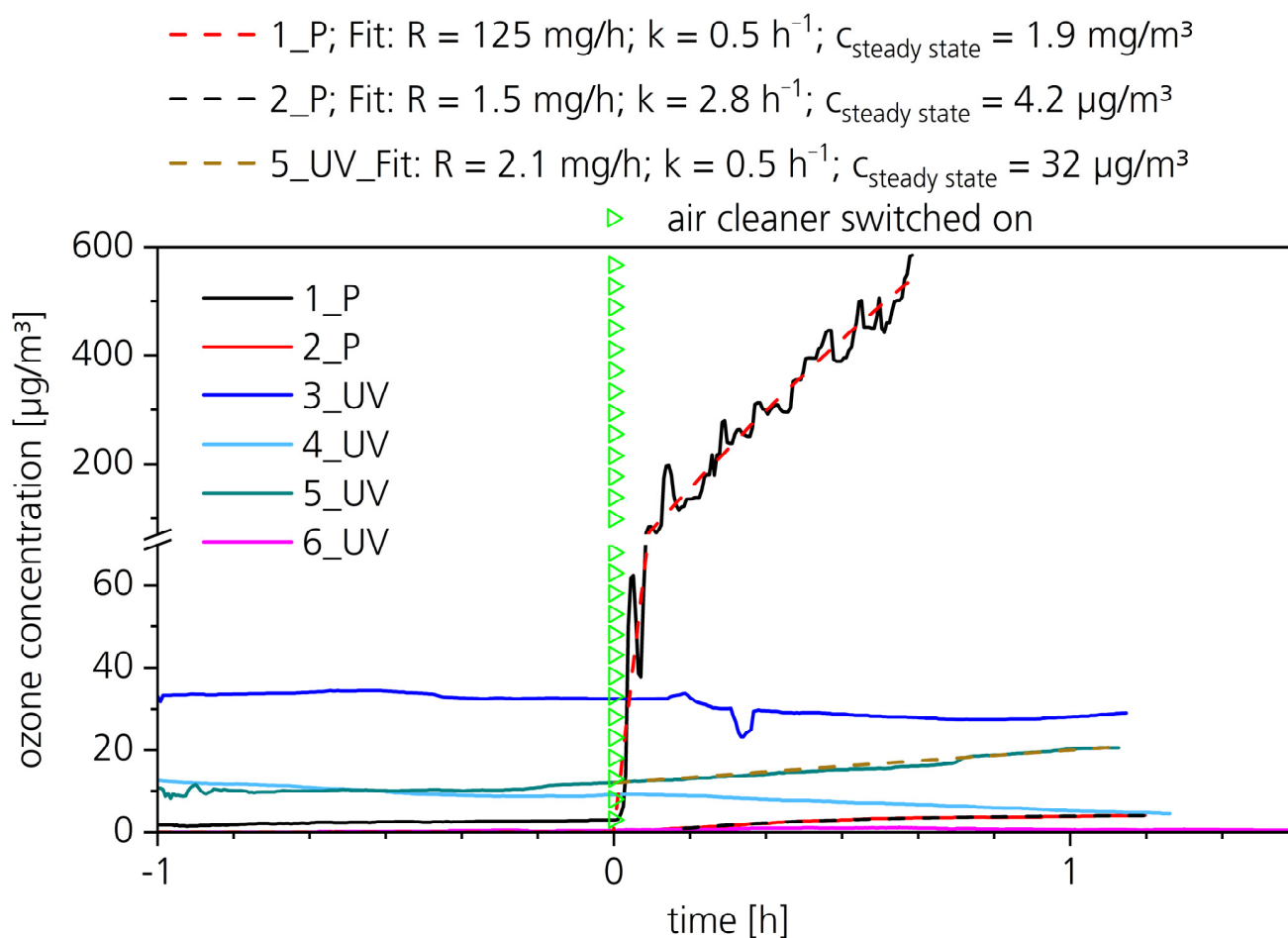


Figure 4. Ozone releases of all air cleaners. In this figure the air cleaners started at $t = 0 \text{ h}$ (green triangle). A concentration decline occurred for the air cleaners 3_UV, 4_UV, and 6_UV. For the air cleaners 1_P, 2_P, and 5_UV, the concentration rise was fitted by the model based on Equation (1), and a steady state concentration for infinite run-time was calculated.

4. Discussion

The devices were selected randomly from those available on the market and represented a wide range of models. Mature devices, regardless of the technology used, should be able to efficiently reduce indoor air contamination with virulent pathogens and, as far as possible, not emit any undesirable substances into the room. It shall be clear to the customer whether the technology offered is based on the separation of virus-containing particles or on the reduction of virulence through disinfection. The absence of a particle separating effect does not allow any conclusions to be drawn regarding the remaining potential virus

infectivity. The results show that the effects of disinfection and filter technologies require separate consideration.

While continuously dosing a functioning air cleaner reduces the concentration rise of either particles or infectious viruses. However, a reduction of 100% cannot occur due to the continuous dosing. In our study, a virulent emitter continuously releases infectious particles. Therefore, the ratio of the steady-state concentration c_{AC} with an active air cleaner to the steady state concentration c_{nat} without an air cleaner can be calculated by Equation (2):

$$\frac{c_{AC}}{c_{nat}} = \frac{k_{nat}}{(k_{nat} + k_{AC})} \quad (2)$$

For instance, with $k_{nat} = 0.5 \text{ h}^{-1}$ and $k_{AC} = 9.5 \text{ h}^{-1}$, a ratio of 1:20 can be reached. For higher natural loss coefficients k_{nat} , the relative effect of the air cleaner decreases and thus the ratio increases (up to 1:1), but nevertheless the absolute steady-state concentration is decreased always when a functioning air cleaner ($k_{AC} > 0$) is used.

4.1. Particle Concentration

The CADR is typically applied to estimate the efficacy of a filtering device in a room. It indicates how many cubic meters of cleaned air the room air cleaner provides per hour and thus corresponds to the filter efficiency and volume flow circulated by the unit. High CADR is a product of high separation efficiency and high air circulation. In the standard, three particle size ranges are mentioned: 0.09–1.0 μm for smoke, 0.5–3 μm for dust, and 5–11 μm for pollen [9,10,53]. The target parameter measured in this study was Phi6 bacteriophage, which falls into the particle range 0.09–1.0 μm . The dosing of the bacteriophage suspension was permanent, in contrast to the punctual dosing according to the standard. Nevertheless, particle concentration curves were calculated based on the air cleaner loss coefficient k_{AC} (near the CADR concept) to illustrate the removal efficiency of the air purification devices.

For the non-separating devices and the devices with coarse filter (devices 1_P, 3_UV, 4_UV and 5_UV), the particle concentration in the room increased continuously. The natural loss coefficient $k_{nat,particles}$ for the particles was in the range between 0.6 and 1.5 h^{-1} . In accordance with Equation (1), the concentration curves converge exponentially toward a steady-state plateau, which could occur after many hours. In the units assembled with an ultra-fine particle filter (2_P and 6_UV), separating effects appeared when the units were in operation.

4.2. Virulence

The final particle concentrations of all inactivating technologies without an efficient filter did not allow any conclusion to be made about the actual infectivity of the virus particles. For this purpose, the air samples were examined for their virulence by a plaque assay. The reduction in virulence showed different results depending on the technology used.

Except for the air cleaner 3_UV, the steady-state concentration was reached already during sampling of the first sample after switching on the air cleaner (P2), indicating a high total loss coefficient.

For filtration devices equipped with an ultra-fine particle filter (2_P and 6_UV), the first sampling, half an hour after the start of operation (P2), was still in the decaying range of the exponential decline curve, whereas the second sampling after about 1 h (P3) occurred when a steady-state was established. For air cleaner 6_UV, utilizing an ultra-fine particle filter, the reduction in virulence represents a combined contribution of filtering and virus-inactivating effects.

Concerning infectious Phi6 phages, the filtering effect of the coarse filter of device 5_UV and the ultra-fine particle filter of device 2_P was negligible. Nevertheless, both devices showed a high Phi6 inactivation efficiency.

For the pure inactivating technologies 1_P and 3_UV, the filtering efficiency was zero or almost zero, but both technologies were effective in reducing the virulence of the Phi6 phages.

4.3. Potential Release of By-Products

With the exception of the pure plasma device 1_P, whose testing was aborted due to safety risks, all investigated air cleaning devices did not form VOCs of concern. The measured concentrations were well below the threshold values. Some of them even reduced the ozone concentration. The technologies investigated are, in principle, able to produce reaction products that pose a health risk. Therefore, it could be assumed that the manufacturers invested increased efforts in the development of the inactivating technologies, such as optimizing electronic control of the plasma units (e.g., pulsed plasma), shaded the ozone producing wavelength below 200 nm of the UVC units, or installing activated carbon filters as absorbents for ozone and VOCs [16,23,67]

Both technologies are also marketed alternatively for indoor air purification from gaseous emissions [34,68]. Therefore, the VOC concentrations in the room were also reduced (except for 1_P). This was confirmed by measuring the initial VOC concentrations in the test room, which were, in some cases, significantly higher than during device operation (data not published). Nevertheless, it was just a coincidence to analyze a huge number of inconspicuous technologies because of receiving higher-priced devices from market.

In order to avoid adverse effects, the high release of ozone by plasma-based air cleaner 1_P and UVC-based device 5_UV demonstrated that a focus on measuring undesired by-products is still necessary for each new released air cleaner. Further insights into the capability of plasma technology of releasing substances of concerns were presented at the Indoor Air Conference 2022 in Kuopio, Finland [69]

5. Conclusions

“Virulence” does not necessarily correlate with the “presence of viruses”. The microbiological detection of viral genetic material confirms the presence of a detectable viral genome but does not indicate the extent of actual infectivity or virulence. The main finding of the investigation was that air cleaning devices on the basis of inactivating technologies need a deeper insight into their efficacy. A sole focus on the particle removal efficiency as required for filtering systems did not lead to satisfactory results because several inactivating devices did not reduce the particle concentration. In contrast, the effect is based on inactivating the capability to infect a host cell. Therefore, a high number of viruses may be present in the room, but they may be harmless because they were inactivated by plasma or UVC technology.

We demonstrated that even in the presence of a strong continuous emitter (“super-spreader event”), efficient inactivating air cleaners could prevent the accumulation of infectious viral aerosol particles and reduce it to a low level (e.g., see Figure 3 for 4_UV with $k_{AC \text{ Phi}6 \text{ min}} 8 \text{ h}^{-1}$ about 10% compared to a situation without an air cleaner can be reached), thus substantially reducing the risk of infection.

In contrary to exponential decay curves (spot dosing), the continuous Phi6-bacteriophage release is advantageous because the natural loss coefficient k_{nat} has only a little influence on the determined air cleaner loss coefficient. The disadvantage of the utilization of continuous Phi6 release is the uncertainty of the plaque assay results usually between 10 and 30%. Nevertheless, the presented results demonstrated the applicability of the test procedure with continuous Phi6 release.

The major shortcoming of the study is the aspect of the air intermixture in the test room. The determined loss coefficients are valid for the location where the measurement or the samplings took place. The distribution of active Phi6 in the room was not considered due to the high effort of the microbiological examinations. Therefore, it could not be assessed if the cleaning efficiency is only a local effect at the point of germ sampling or if the whole room air is cleaned. Nevertheless, we wanted to conduct investigations under realistic conditions rather than determine clean air delivery rates according to the existing standards. In general, the experimental results show that there is currently no measurement that correctly describes the effect to the entire room. Investigations to obtain higher spatial resolutions are necessary.

Author Contributions: A.B.-F.: Conceptualization, Writing—Original draft preparation; M.B.: Methodology, Investigation, Formal analysis and Visualization; G.G.: Supervision, Funding Acquisition; W.K.H.: Conceptualization, Methodology; S.J.: Project administration, Resources; A.M.N.-R.: Methodology, Investigation, Validation and Formal analysis; C.R.S.: Supervision and Funding Acquisition; A.S.: Formal analysis and Validation. All authors have read and agreed to the published version of the manuscript.

Funding: The study was financed by the action program “Fraunhofer vs. Corona”, conducted within the research project “Hy4HoGa”, funded by the Bavarian State Ministry for Economic Affairs (funding code 75-4882/119/1), Regional Development and Energy and the project “Testaerosole” funded by the Ministry of Science, Research and the Arts Baden-Württemberg under the special funding line “COVID-19 Research–Health Air Initiative” (funding code 017/100241).

Data Availability Statement: The data were all generated at the Fraunhofer IBP. Details about the manufacturers are subject to confidentiality.

Conflicts of Interest: The authors declare no conflict of interest. The funders had no role in the design of the study; in the collection, analyses, or interpretation of data; in the writing of the manuscript; or in the decision to publish the results.

References

- Enjuanes, L.; Smerdou, C.; Castilla, J.; Anton, I.M.; Torres, J.M.; Sola, I.; Golvano, J.; Sanchez, J.M.; Pintado, B. Development of protection against coronavirus induced diseases. A review. *Adv. Exp. Med. Biol.* **1995**, *380*, 197–204. [PubMed]
- Graham, R.L.; Baric, R.S. Recombination, reservoirs, and the modular spike: Mechanisms of coronavirus cross-species transmission. *J. Virol.* **2010**, *84*, 3134–3146. [CrossRef] [PubMed]
- Fehr, A.R.; Perlman, S. Coronaviruses: An overview of their replication and pathogenesis. *Methods Mol. Biol.* **2015**, *1282*, 1–23.
- Cui, J.; Li, F.; Shi, Z.L. Origin and evolution of pathogenic coronaviruses. *Nat. Rev. Microbiol.* **2019**, *17*, 181–192. [CrossRef]
- Liu, L.; Wang, P.; Nair, M.S.; Yu, J.; Rapp, M.; Wang, Q.; Luo, Y.; Chan, J.F.; Sahi, V. Potent neutralizing antibodies against multiple epitopes on SARS-CoV-2 spike. *Nature* **2020**, *584*, 450–456. [CrossRef] [PubMed]
- Melanthota, S.K.; Banik, S.; Chakraborty, I.; Pallen, S.; Gopal, D.; Chakrabarti, S.; Mazumder, N. Elucidating the microscopic and computational techniques to study the structure and pathology of SARS-CoVs. *MRT* **2020**, *83*, 1623–1638. [CrossRef] [PubMed]
- Fennelly, K.P. Particle sizes of infectious aerosols: Implications for infection control. *Lancet Respir. Med.* **2020**, *8*, 914–924. [CrossRef]
- GAeF Association for Aerosol Research. Position Paper of the Gesellschaft für Aerosolforschung on Understanding the Role of Aerosol Particles in SARS-CoV-2 Infection, Issue 17 December 2020. Available online: https://www.info.gaef.de/_files/ugd/fab12b_0b691414cfb344fe96d4b44e6f44a5ab.pdf (accessed on 1 August 2022).
- Küpper, M.; Asbach, C.; Schneiderwind, U.; Finger, H.; Spiegelhoff, D.; Schumacher, S. Testing of an Indoor Air Cleaner for Particulate Pollutants under Realistic Conditions in an Office Room. *Aerosol. Air Qual. Res.* **2019**, *19*, 1655–1665. [CrossRef]
- Curtius, J.; Granzin, M.; Schrod, J. Testing mobile air purifiers in a school classroom: Reducing the airborne transmission risk for SARSCoV-2. *Aerosol Sci. Technol.* **2021**, *55*, 586–599. [CrossRef]
- Cimolai, N. Environmental and decontamination issues for human coronaviruses and their potential surrogates. *J. Med. Virol.* **2020**, *92*, 2498–2510. [CrossRef]
- Chin, A.W.H.; Chu, J.T.S.; Perera, M.R.A.; Hui, K.P.Y.; Yen, H.-L.; Chan, M.C.W.; Peiris, M.; Poon, L.L.M. Stability of SARS-CoV-2 in different environmental conditions. *Lancet Microbe* **2020**, *1*, 1. [CrossRef]
- Jiang, J.; Fu, Y.V.; Liu, L.; Kulmala, M. Transmission via aerosols: Plausible differences among emerging coronaviruses. *Aerosol Sci. Technol.* **2020**, *54*, 865–868. [CrossRef]
- Assadi, I.; Guesmi, A.; Baaloudj, O.; Zeghioud, H.; Elfalleh, W.; Benhammadi, N.; Khezami, L.; Assadi, A.A. Review on inactivation of airborne viruses using non-thermal plasma technologies: From MS2 to coronavirus. *ESPR* **2022**, *29*, 4880–4892. [CrossRef] [PubMed]
- Snelling, W.J.; Afkhami, A.; Turkington, H.L.; Carlisle, C.; Cosby, S.L.; Hamilton, J.W.J.; Ternan, N.G.; Dunlop, P.S.M. Efficacy of single pass UVC air treatment for the inactivation of coronavirus, MS2, coliphage and Staphylococcus aureus bioaerosols. *J. Aerosol Sci.* **2022**, *164*, 106003. [CrossRef]
- Thornton, G.M.; Fleck, B.A.; Fleck, N.; Kroeker, E.; Dandnyak, D.; Zhong, L.; Hartling, L. The impact of heating, ventilation, and air conditioning design features on the transmission of viruses, including the 2019 novel coronavirus: A systematic review of ultraviolet radiation. *PLoS ONE* **2022**, *17*, e0266487. [CrossRef]
- VDI EE 4300-14:2021-09; Messen von Innenraumluftverunreinigungen—Blatt 14: Anforderungen an Mobile Luftreiniger zur Reduktion der aerosolgebundenen Übertragung von Infektionskrankheiten. VDI/DIN-Kommission Reinhaltung der Luft (KRdL) – Normenausschuss: Düsseldorf, Germany, 2021.
- Terrier, O.; Essere, B.; Yver, M.; Barthelemy, M.; Bouscambert-Duchamp, M.; Kurtz, P.; Van Mechelen, D.; Morfin, F.; Billaud, G.; Ferraris, O.; et al. Cold oxygen plasma technology efficiency against different airborne respiratory viruses. *J. Clin. Virol.* **2009**, *45*, 119–124. [CrossRef]

19. Thirumdas, R.; Sarangapani, C.; Annapure, U.S. Cold Plasma A novel Non-Thermal Technology for Food Processing. *Food Biophys.* **2015**, *10*, 1–11. [[CrossRef](#)]
20. Lai, A.C.K.; Cheung, A.C.T.; Wong, M.M.L.; Li, W.S. Evaluation of cold plasma inactivation efficacy against different airborne bacteria in ventilation duct flow. *Build Environ.* **2016**, *98*, 39–46. [[CrossRef](#)]
21. Niedzwiedz, I.; Wasko, A.; Pawlat, J.; Polak-Berecka, M. The State of Research on Antimicrobial Activity of Cold Plasma. *PJM* **2019**, *68*, 153–164. [[PubMed](#)]
22. Ehlbeck, J.; Schnabel, U.; Polak, M.; Winter, J.; Won Woedtke, T.; Brandenburg, R.; von dem Hagen, T.; Weltmann, K.D. Low temperature atmospheric pressure plasma sources for microbial decontamination. *J. Phys. D Appl. Phys.* **2010**, *44*, 013002. [[CrossRef](#)]
23. Bahri, M.; Haghghat, F. Plasma-Based Indoor Air Cleaning Technologies: The State of the Art-Review. *Clean* **2014**, *42*, 1667–1680. [[CrossRef](#)]
24. Puligundla, P.; Mok, C. Non-thermal plasmas (NTPs) for inactivation of viruses in abiotic environment. *Res. J. Biotech.* **2016**, *11*, 91–96.
25. Weiss, M.; Daeschlein, G.; Kramer, A.; Burchardt, M.; Brucker, S.; Wallwiender, D.; Stope, M.B. Virucide properties of cold atmospheric plasma for future clinical applications. *J. Med. Virol.* **2016**, *89*, 952–959. [[CrossRef](#)] [[PubMed](#)]
26. Filipic, A.; Primc, G.; Zaplotnik, R.; Mehle, N.; Gutierrez-Aguirre, I.; Ravnikar, M.; Mozetic, M.; Zel, J.; Dobnik, D. Cold Atmospheric Plasma as a Novel Method for Inactivation of Potato Virus Y in Water Samples. *Food Environ. Virol.* **2019**, *11*, 220–228. [[CrossRef](#)] [[PubMed](#)]
27. Wu, Y.; Liang, Y.; Wei, K.; Yao, M.; Zahng, J.; Grinshpun, S.A. MS2 Virus Inactivation by Atmospheric-Pressure Cold Plasma Using Different Gas Carriers and Power Levels. *Appl. Environ. Microbiol.* **2015**, *81*, 996–1002. [[CrossRef](#)] [[PubMed](#)]
28. Xia, T.; Kleinheksel, A.; Lee, E.M.; Qiao, Z.; Wigginton, K.R.; Clack, H.L. Inactivation of airborne viruses using a packed bed non-thermal plasma reactor. *J. Phys. D Appl. Phys.* **2019**, *52*, 255201. [[CrossRef](#)]
29. Bisag, A.; Isabelli, P.; Laurita, R.; Bucci, C.; Capelli, F.; Dirani, G.; Gherardi, M.; Laghi, G.; Paglianti, A.; Sambri, V.; et al. Cold atmospheric plasma inactivation of aerosolized microdroplets containing bacteria and purified SARS-CoV-2 RNA to contrast airborne transmission. *Plasma Process Polym.* **2020**, *17*, e2000154. [[CrossRef](#)]
30. Jakober, C.; Phillips, T. *Evaluation of Ozone Emissions from Portable Indoor Air Cleaners: Electrostatic Precipitators and Ionizers*; Staff Technical Report; Air Resources Board of the California Environmental Protection Agency: Sacramento, CA, USA, 2008.
31. Zimmermann, J.L.; Dumler, K.; Shimizu, T.; Morfill, G.E.; Wolf, A.; Boxhammer, V.; Schlegel, J.; Gansbacher, B.; Anton, M. Effects of cold atmospheric plasmas on adenoviruses in solution. *J. Phys. D Appl. Phys.* **2011**, *44*, 505201. [[CrossRef](#)]
32. Preis, S.; Klauson, D.; Gregor, A. Potential of electric discharge plasma method in abandonment of volatile organic compounds originating from the food industry. *J. Environ. Manag.* **2013**, *114*, 125–138. [[CrossRef](#)]
33. Liao, X.; Liu, D.; Xiang, Q.; Ahn, J.; Chen, S.; Ye, X.; Ding, T. Inactivation mechanisms of non-thermal plasma on microbes: A review. *Food Control* **2017**, *75*, 83–91. [[CrossRef](#)]
34. Prehn, F.; Timmermann, E.; Kettlitz, M.; Schaufler, K.; Günther, S.; Hahn, V. Inactivation of airborne bacteria by plasma treatment and ionic wind for indoor air cleaning. *Plasma Prog. Polym.* **2020**, *17*, e2000027. [[CrossRef](#)]
35. Jagger, J. Introduction to Research in Ultraviolet Photobiology. *Photochem. Photobiol.* **1968**, *7*, 413.
36. Budowsky, E.I.; Bresler, S.E.; Friedman, E.A.; Zheleznova, N.V. Principles of selective inactivation of viral genome. I. UV-induced inactivation of influenza virus. *Arch. Virol.* **1981**, *68*, 239–247. [[CrossRef](#)]
37. Walker, C.M.; Ko, G. Effect of ultraviolet germicidal irradiation on viral aerosols. *Environ. Sci. Technol.* **2007**, *41*, 5460–5465. [[CrossRef](#)] [[PubMed](#)]
38. Kowalski, W. *Ultraviolet Germicidal Irradiation Handbook. UVGI for Air and Surface Disinfection*; Springer: Berlin/Heidelberg, Germany, 2009; 501p.
39. Sellera, F.P.; Sabino, C.P.; Cabral, F.V.; Ribeiro, M.S. A systematic scoping review of ultraviolet C (UVC) light systems for SARS-CoV-2 inactivation. *Photochem. Photobiol.* **2021**, *8*, 100068. [[CrossRef](#)]
40. Heßling, M.; Hönes, K.; Vatter, P.; Lingenfelder, C. Ultraviolette Bestrahlungsdosen für die Inaktivierung von Coronaviren—Review und Analyse von Coronavirusinaktivierungsstudien. *GMS Hyg. Infect. Control* **2020**, *15*, 1–8.
41. Watts, S.; Ramstedt, M.; Salentinig, S. Ethanol Inactivation of Enveloped Viruses: Structural and Surface Chemistry Insights into Phi6. *J. Phys. Chem. Lett.* **2021**, *12*, 9557–9563. [[CrossRef](#)]
42. King, A.M.Q.; Lefkowitz, E.J.; Adams, M.J.; Carstens, E.B. *Virus Taxonomy. Classification and Nomenclature of Viruses, Ninth Report of the International Committee on Taxonomy of Viruses*; International Committee on Taxonomy of Viruses: Moscow, Russia, 2012; pp. 515–518.
43. Aquino de Carvalho, N.; Stachler, E.N.; Cimabue, N.; Bibby, K. Evaluation of Phi6 Persistence and Suitability as an Enveloped Virus Surrogate. *Environ. Sci. Technol.* **2017**, *51*, 8692–8700. [[CrossRef](#)] [[PubMed](#)]
44. Cadnum, J.L.; Li, D.F.; Jones, L.D.; Redmond, S.N.; Pearlmutter, B.; Wilson, B.M.; Donskey, C.J. Evaluation of Ultraviolet-C Light for Rapid Decontamination of Airport Security Bins in the Era of SARS-CoV-2. *Pathog. Immun.* **2020**, *5*, 133–142. [[CrossRef](#)]
45. Silverman, A.I.; Boehm, A.B. Systematic Review and Meta-Analysis of the Persistence and Disinfection of Human Coronaviruses and Their Viral Surrogates in Water and Wastewater. *Environ. Sci. Technol. Lett.* **2020**, *7*, 544–553. [[CrossRef](#)]
46. Tseng, C.C.; Li, C.L. Inactivation of Virus-Containing Aerosols by Ultraviolet Germicidal Irradiation. *Aerosol Sci. Technol.* **2005**, *39*, 1136–1142. [[CrossRef](#)]

47. Adcock, N.J.; Rice, E.W.; Sivaganesan, M.; Brown, J.D.; Stallknecht, D.E.; Swayne, D.E. The use of bacteriophages of the family Cystoviridae as surrogates for H5N1 highly pathogenic avian influenza viruses in persistence and inactivation studies. *J. Environ.* **2009**, *44*, 1362–1366.
48. Turgeon, N.; Toulouse, M.-J.; Martel, B.; Molneau, S.; Duchaine, C. Comparison of Five Bacteriophages as Models for Viral Aerosol Studies. *Appl. Environ.* **2014**, *80*, 4242–4250. [[CrossRef](#)] [[PubMed](#)]
49. Ford, B.E. Pseudomonas Bacteriophage Phi6 as a Model for Virus Emergence. Ph.D. Thesis, Graduate Center, City University of New York, New York, NY, USA, 2015.
50. Prussin, A.J.; Schwake, D.O.; Lin, K.; Gallagher, D.L.; Buttlng, L.; Marr, L.C. Survival of the Enveloped Virus Phi6 in Droplets as a Function of Relative Humidity, Absolute Humidity, and Temperature. *Appl. Environ.* **2018**, *84*, e00551-18. [[CrossRef](#)] [[PubMed](#)]
51. Blatchley, E.R., III; Petri, B.; Sun, W. SARS-CoV-2 Dose-Response Behavior. White Paper Prepared for UV-A 2020. 6p. Available online: <https://iuva.org/resources/covid-19/SARS%20CoV2%20Dose%20Response%20White%20Paper.pdf> (accessed on 1 August 2022).
52. Fedorenko, A.; Grinberg, M.; Orevi, T.; Kashtan, N. Survival of the enveloped bacteriophage Phi6 (a surrogate for SARS-CoV-2) in evaporated saliva microdroplets deposited on glass surfaces. *Sci. Rep.* **2020**, *10*, 1–10. [[CrossRef](#)] [[PubMed](#)]
53. AHAM AC-1:2020-00; Method for Measuring Performance of Portable Household Electric Room Air Cleaners. Association of Home Appliance Manufacturers: Washington, DC, USA, 2020.
54. Schmohl, A.; Nagele-Renzl, A.M.; Scherer, C.R.; Buschhaus, M.; Hofbauer, W.; Johann, S.; Burdack-Freitag, A.; Grün, G. Determination of CADR of virus-inactivating air purifiers by surrogate virus plaque assay. Indoor Air 2022. In Proceedings of the 17th International Conference of the International Society of Indoor Air Quality & Climate, Kuopio, Finland, 12–16 June 2022; p. 1204.
55. Schumacher, S.; Asbach, C.; Schmid, H.-J. Effektivität von Luftreinigern zur Reduzierung des COVID-19-Infektionsrisikos/Efficacy of air purifiers in reducing the risk of COVID-19 infections. *GrdL (Gefahrstoffe)* **2021**, *81*, 16–28. [[CrossRef](#)]
56. Jung, H. Modeling CO2 Concentrations in Vehicle Cabin. SAE Technical Paper 2013-01-1497. 2013, pp. 1–6. Available online: <https://www.sae.org/publications/technical-papers/content/2013-01-1497/> (accessed on 1 August 2022).
57. Hershey, A.D.; Kalmanson, G.; Bronfenbrenner, J. Quantitative Methods in the Study of the Phage-Antiphage Reaction. *J. Immunol.* **1943**, *46*, 267–279.
58. Kropinski, A.M.; Mazzocco, A.; Waddell, T.E.; Lingohr, E.; Johnson, R.P. Enumeration of Bacteriophages by Double Agar Overlay Plaque Assay. In *Bacteriophages: Methods and Protocols, Volume I: Isolation, Characterization, and Interactions. Methods in Molecular Biology*; Clokie, M.R.J., Kropinsky, A.M., Eds.; Humana Press: Totowa, NJ, USA; Springer Science+Business Media: New York, NY, USA, 2009; pp. 69–76.
59. Baer, A.; Kehn-Hall, K. Viral Concentration Determination Through Plaque Assay: Using Traditional and Novel Overlay Systems. *J. Vis. Exp.* **2014**, *93*, 1–10. [[CrossRef](#)]
60. EN 13610:2002-10; Chemical Disinfectants—Quantitative Suspension Test for the Evaluation of Virucidal Activity against Bacteriophages of Chemical Disinfectants Used in Food and Industrial Areas—Test Method and Requirements (Phase 2, Step 1). European Committee for Standardization (CEN): Brussels, Belgium, 2002.
61. Govindarajulu, Z. *Statistical Techniques in Bioassay, 2nd Revised and Enlarged Edition*; Karger: New York, NY, USA, 2001.
62. EN ISO 16000-1:2006; Indoor Air—Part 1: General Aspects of Sampling Strategy. Kommission Reinhaltung der Luft (KRdL) im VDI und DIN – Normenausschuss: Düsseldorf, Germany, 2006.
63. EN 16516:2017+A1:2020; Construction Products: Assessment of Release of Dangerous Substances—Determination of Emissions into Indoor Air. VDI/DIN-Kommission Reinhaltung der Luft (KRdL)–Normenausschuss: Düsseldorf, Germany, 2020.
64. UBA Umweltbundesamt. Einsatz Mobiler Luftreiniger als Lüftungsunterstützende Maßnahme in Schulen Während der SARS-CoV-2 Pandemie. Stellungnahme der Kommission Innenraumlufthygiene (IRK). Available online: https://www.umweltbundesamt.de/sites/default/files/medien/2546/dokumente/201116_irk_stellungnahme_luftreiniger.pdf (accessed on 1 August 2022).
65. ECDC European Center for Disease Prevention and Control. Heating, Ventilation and Air Conditioning Systems in the Context of COVID-19. First Update. Available online: <https://www.ecdc.europa.eu/sites/default/files/documents/Ventilation-in-the-context-of-COVID-19.pdf> (accessed on 1 August 2022).
66. AgBB—Committee for Health-related Evaluation of Building Products: Requirements for the Indoor Air Quality in Buildings: Health-related Evaluation Procedure for Emissions of Volatile Organic Compounds (VVOC, VOC and SVOC) from Building Products. Version 2021. Available online: https://www.umweltbundesamt.de/sites/default/files/medien/4031/dokumente/agbb_bewertungsschema_2021.pdf (accessed on 1 August 2022).
67. Raeiszadeh, M.; Adeli, B. A Critical Review on Ultraviolet Disinfection Systems against COVID-19 Outbreak: Applicability, Validation, and Safety Considerations. *ACS Photonics* **2020**, *7*, 2941–2951. [[CrossRef](#)]
68. Asilevi, P.J.; Boakye, P.; Oduro-Kwarteng, S.; Fei-Baffoe, B.; Sokama-Neuyam, Y.A. Indoor air quality improvement and purification by atmospheric pressure Non-Thermal Plasma (NTP). *Sci. Rep.* **2021**, *11*, 22830. [[CrossRef](#)] [[PubMed](#)]
69. Burdack-Freitag, A.; Buschhaus, M.; Nagele-Renzl, A.; Hofbauer, W.; Johann, S.; Scherer, C.R.; Schmohl, A.; Grün, G. Release of undesired by-products during the operation of virus inactivating air cleaning devices. Indoor Air 2022. In Proceedings of the 17th International Conference of the International Society of Indoor Air Quality & Climate, Kuopio, Finland, 12–16 June 2022; p. 1195.